Improvement of the electrolytic metal pickling process by inter-electrode insulation

N. Ipek[1], N. Lior*[2] and A. Eklund[3]

The existing industrial electrolytic steel pickling process is only 30% current efficient. Use of approximate modelling of the process and solution of the model predicts that inter-electrode insulation improves the current and energy efficiency, and this paper describes the experimental work that has validated this prediction. Some of the main results are: (a) the current efficiency varied from 20% without insulation to 100% with complete insulation, (b) the use of just partial insulations yielded a significant improvement in the process efficiency and at the same time maintained good electrolyte mixing and homogeneity which can not be attained with complete insulation. The theoretical foundations of this method and its various consequences are discussed. The method is relatively easy to apply to existing industrial electrolytic pickling tanks, and also provides system control flexibility for optimal pickling of different steel grades. The method's application cost is relatively low and saves investment in new equipment if a retrofit of an existing system is desired.

Keywords: Steels, Pickling, Efficiency, Insulation

Introduction

In the production process of stainless steel bands, the steel is rolled, annealed and subjected to pickling several times until the desired thickness and surface properties are attained. In general the steel is hot rolled at 1250°C until the thickness of the slab is reduced to about 5–25 mm[1] and then cold rolled at room temperature until the desired final thickness is attained.

The thermal conditions during hot rolling lead to the undesirable formation of oxide scale, about 50–500 μm thick, on the steel surfaces.[1] This rolling scale is usually composed of a mixed iron and chromium oxide, also referred to as a spinel. Furthermore, rolling alters the crystal structure and microstructures of the steel, i.e. the material increases in strength. Therefore, to soften the steel and restore the desired crystal structure and microstructure, it is generally subjected to an annealing treatment for a few minutes in a furnace where the oxygen partial pressure is controlled. The treatment requires temperatures in the furnace of about 800–900°C for ferrites and 1200°C for austenites.[2] Prior to the annealing process the steel band is cooled and shot blasted, removing most of the oxide. However, because of the thermal conditions during the annealing treatment in the annealing and pickling line the surface is further oxidised and normally a region depleted in chromium appears below the oxide layer. It is stated[3] that the formation of mixed chromium oxides and the chromium depleted region occur as a result of the diffusion of the chromium to the surface and its high affinity to combine with oxygen into a stable oxide. Both the scale and the chromium depleted region do not have the desired corrosion resistant properties and must therefore be removed, before the steel band can be subjected to further rolling.

The oxide scale on hot rolled steel bands is reported[2] to be made up mostly of iron oxides but also some chromium rich oxides. In general such an oxide is removed by shot blasting and/or brushing in order to uncover a sufficient area of the chrome depleted region or the steel matrix, whereby a fast pickling rate is achieved in the subsequent electrolytic and acid pickling. The general opinion is that the acids penetrate the obtained cracks and thereby dissolve the chromium depleted region. Consequently the oxide scale loosens from the steel surface. However, the electrolytic pickling efficiency with shot blasted steel bands was reported to be 20–30%.[2]

Thereafter, when the aim is to produce thinner steel bands, cold rolling at room temperature is performed. Cold rolling, similarly to hot rolling, hardens the material. Therefore the steel band is annealed again, during which a mixed oxide, about 10 μm thick, forms on the surface of the steel band. To remove this oxide scale the steel band is subjected to subsequent treatments of neutral, electrolytic and mixed acid pickling. When cold rolled steel bands are processed, shot blasting is replaced by electrolytic pickling to avoid damaging the surface.

It is generally agreed[5–8] that the mechanism of electrolytic pickling is electrochemical dissolution in

[1]Faxénlaboratoriet, Department of Mechanics, Kungliga Tekniska Högskolan, 100 44 Stockholm, Sweden
[2]Department of Mechanical Engineering and Applied Mechanics, University of Pennsylvania, Philadelphia, PA 19104–6315, USA
[3]AvestaPolarit AB, SE–77480 Avesta, Sweden

*Corresponding author, e-mail lior@seas.upenn.edu

Published by Maney on behalf of the Institute
Received 16 December 2003; accepted 6 September 2004
DOI 10.1179/174328105X23996

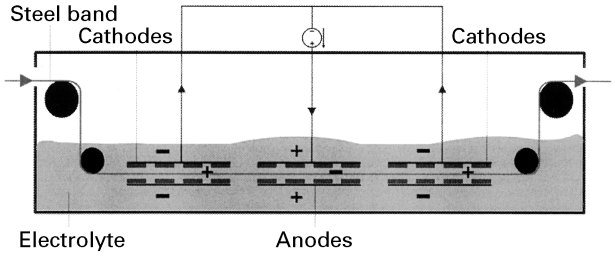

1 Illustration of electrolytic pickling tank of Ruthner Neolyte process,[9] with one out of four typical electrode assemblies placed symmetrically above and below the moving steel band: at each end there is a set of four cathodes and in the centre a set of four anodes

the transpassive region of the steel, i.e. the passage of current through the steel band results in electrochemical dissolution of the actual oxide scale, and that the benefit of this process is the oxidation of Cr(III) in the hard to dissolve Cr_2O_3 oxide to Cr(VI), which yields easily soluble compounds. It has also been stated[4] that the main mechanism is electrochemical dissolution of the chromium depleted layer underlying the scale, whereby the scale is loosened from the steel surface.

A typical electrolytic pickling tank for the Ruthner process,[9] shown in Fig. 1, contains a conducting neutral aqueous solution of sodium sulphate (Neolyte), which reduces the use of aggressive and environmentally hostile acids. Throughout the tank there are four identical electrode configurations, similar to the one illustrated in Fig. 1. Each configuration is made up of three electrode groups, four cathodes at the start and end and four anodes in the centre, and is run by a separate power supply (typically at 10 kV each). The electric current (typically, for cold rolled steel, 0·8–1 kA m^{-2}), flows from the anodes through the electrolyte onto and through the moving steel band and then back to the cathodes through the electrolyte. This way the steel band becomes polarised anodically opposite to the cathodes and cathodically opposite to the anodes without direct electrical contact with the electrodes.

With these types of process configurations, it was observed that a significant amount of the current does not reach the steel band intended to be treated, but short-circuits between electrodes of different polarity, as is shown in Fig. 2, which was obtained from the authors' process model described in detail in Ref. 10.

This model solves the Laplace partial differential equation for the electric potential in the electrolyte and electrodes, subjected to nonlinear boundary kinetics for the electrode reactions and prescribed potential on the top surfaces of the anodes/cathodes. The anode/cathode current densities associated with the oxygen/hydrogen evolution are expressed by the Tafel laws, owing to the high anodic/cathodic over potentials. Here the steel band is treated as a bipolar electrode with induced potential, which is calculated as part of the mathematical solution. At the interfaces between the electrodes/electrolyte and steel band/electrolyte continuity of the normal current density is prescribed. In addition at the insulated parts of the cell, the normal transport rate (current) was set to zero. The effect of gas production on the reduction of the electrolyte conductivity was taken into account by the Bruggemans equation. The

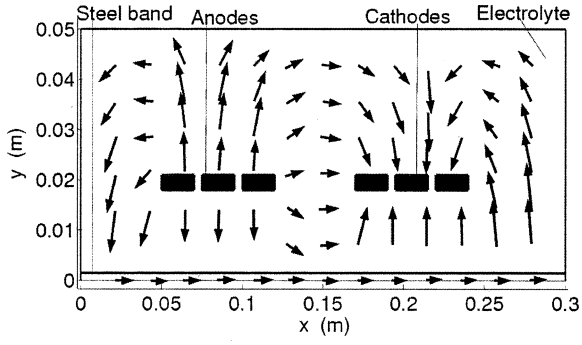

2 Current fields in electrolyte and steel band as calculated from numerical model,[10] under conditions of the experiment (specified in Table 1): note that *y* scale is expanded in the figure relative to *x* scale to provide a better view of the current flow, and the arrows indicate only current flow direction (not magnitude); the undesirable short circuiting between the anodes and cathodes is clearly seen in the centre

implementation of electrode kinetics (Tafel law) in the model, made it possible to estimate the process current efficiency, i.e. the amount of current passing into the steel band compared to the total current applied at the anodes.

The model was solved numerically by using the finite element program FEMLAB. The mesh size was chosen to avoid grid dependence of the solution. It was found[10] that the current efficiency computed by the numerical model agreed with the experimental results qualitatively in exhibiting the same trend and the model predictions showed strong sensitivity to the rate constants. Using a typical work station computer (Sun Ultra 2200 MHz), a typical case using 11 533 elements took 350 CPU seconds to complete.

With the application of complete electrical insulation between the anodes and cathodes, as shown in Fig. 3, this model predicts that the short-circuiting between the electrodes is prevented, forcing the total current into the steel band and increasing the current density at the steel band surface and consequently the pickling rate. This theoretical finding was then followed up by the experimental investigations reported in this paper.

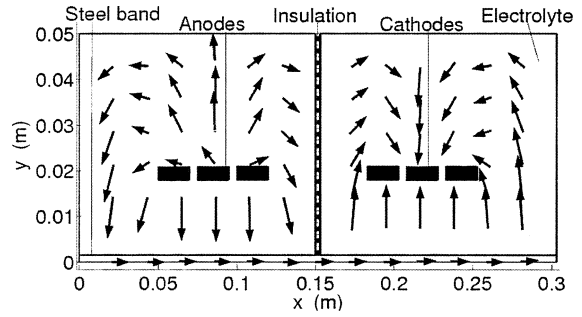

3 Numerical model prediction (*see* Ref. 10) of the current field in the electrolyte and steel band, with the inter-electrode insulation in place: variables used are specified in Table 1; note that *y* scale is expanded in figure relative to the *x* scale to provide a better view of the current flow and the arrows indicate only current flow direction (not magnitude); note also that short circuiting between the anodes and cathodes is prevented by the insulation

Electrolytic pickling processes used commercially have been reported to have a current efficiency χ of about 30%,[11,12] where χ is defined as the ratio of the current passing through the steel band I_B (A) to the total current I_T (A) applied to the system

$$\chi = I_B / I_T \quad (1)$$

A 'Nomenclature' of the symbols used in this paper is given in the Appendix below.

To achieve the desired pickling effect at such a low current efficiency necessitates either the application of high voltages to the electrodes or lowering of the throughput speed of the steel band through the continuous annealing and pickling line. The outcome is either a significant energy loss or a reduced process throughput, which altogether increases capital and operating costs.

We note that the current, passing through the steel band is not solely used for oxide scale dissolution. In bipolar pickling using aqueous electrolytes, it is well known (cf. Refs. 4–7) that electrolysis producing oxygen gas on the anodic section of the steel band described by the reaction

$$2H_2O \rightarrow O_2 + 4H^+ + 4e^- \quad (2)$$

occurs in parallel with the electrochemical dissolution reactions of the oxide. A possible dissolution reaction is[13]

$$Cr_2O_3 + 4H_2O \rightarrow Cr_2O_7^{2-} + 8H^+ + 6e^- \quad (3)$$

at high overpotentials. It was reported in[14] that chromium oxide oxidises to yield the negative dichromate ion in reaction (3). In addition, electrochemical dissolution of the steel base metal is also reported to consume some of the current passing through the steel band

$$Fe \rightarrow Fe^{3+} + 3e^- \quad (4)$$

This additional effect further reduces the process efficiency. The oxygen gas production reaction is reported[7,15] to consume a significant amount of the current that passes into the steel band and is therefore highly undesirable. Although no specific number has been found in the literature, it is stated[15] that more than half of the supplied current is consumed by gas production in electrolytic acid pickling.

On the cathodic section of the steel band, hydrolysis yields hydrogen gas

$$2H_2O + 2e^- \rightarrow H_2 + 2OH^- \quad (5)$$

For each of these electrochemical reactions to occur, the surface of the steel band needs to acquire a certain voltage E (the potential difference between the electrode potential, i.e. the local potential at the steel band surface, and the adjacent potential of the electrolyte solution), which exceeds the equilibrium potential E_0 specific to each reaction. The difference between these voltages is defined as the overpotential $\eta_S = E - E_0$, which is the driving force of an electrochemical reaction. The strength of the surface overpotential depends on the current density at the specific surface. For the oxygen evolution reaction, equation (2), the equilibrium potential is $E_{0,O_2} = 1{\cdot}23 - 0{\cdot}059$ pH (V) at 25°C, for the chromium oxide dissolution reaction, equation (3), it is somewhat simplified, $E_{0,Cr_2O_3} = 1{\cdot}168 - 0{\cdot}0788$ pH (V) and for the base metal iron dissolution reaction, equation (4), the equilibrium potential is $E_{0,Fe} = -0{\cdot}037 + 0{\cdot}0197 \log[Fe^{3+}]$ (V).[13] Therefore, when not taking the kinetics of these reactions into consideration, one can conclude that the acquired surface overpotential can either be above or below the onset voltage for any of the reactions (2), (3) or (4) for a particular current density at the steel band surface.

Dissolution of the oxide scale and steel base in neutral electrolytic pickling is reported[5–7] to occur in the transpassive region of the steel. This region is characterised by the reactivation of the surface, i.e. high anodic current densities, because the steel surface goes from being inert to active. Furthermore the anodic current density at the steel band surface is proportional to the dissolution rate of the oxide and steel base. The measured anodic surface overpotential was reported[5] to be about 2 V *v.* SHE (i.e. with reference to a standard hydrogen electrode), which corresponds to values well above those required to drive reactions (2)–(4). Consequently, although somewhat simplified here, the reactions (2) and (3) will occur simultaneously whereby part of the current provided for oxide dissolution will be consumed by the parallel, and unwanted, oxygen production and probably metal dissolution reactions other than those of Fe. However, each reaction rate depends on the specific kinetics of each reaction. In reality, the electrochemical reactions that occur are of a much more complicated nature than described above.

Apart from the energy penalty, production of oxygen and hydrogen bubbles also insulates the electrodes partially and reduces the electrolyte conductivity, therefore decreasing the process efficiency further. It is noteworthy that it is stated in the literature,[5,11,16] although not proven, that the growing gas bubbles tend to lift the scale mechanically, i.e. peel it off the steel surface. Production of gas is therefore stated to also be of some benefit to the process. The production of oxygen gas creates local turbulence, which increases the rate of diffusion of metal ions away from the surface and prevents the formation of electrochemically generated smut (metal oxides or metal salts that precipitate on the metal surface when the solubility limit of the metal is exceeded at the surface).[17] In addition the production of protons from reaction (2) lowers the pH at the steel band surface, increasing the solubility limit for the metal ions at the surface of the steel band, which also prevents the formation of smut. Furthermore, dissolved metal ions that remain on the steel surface and are not swept away fast enough, oppose thereby the interfacial diffusion process. They can also contaminate the band surface when they precipitate as an oxide or salt as the surface turns cathodically polarised, as a result of the increase in pH at the surface of the steel because of the hydroxyl ions generated by reaction (5). The greater the cathodic current density on the steel surface, the greater the volume of hydroxyl ions produced per unit area and the higher the pH on the surface.

An alternative method to bipolar pickling with anodes and cathodes in the same pickling tank is to place the anodes and cathodes in separate pickling tanks to prevent the current from short circuiting between electrodes of different polarity.[17,18] The disadvantage of such complete separation of the electrodes is,

however, that no mixing of the electrolyte would take place between the different compartments, yielding an inhomogeneous electrolyte solution and an undesirable change in the electrochemistry of the electrolytic pickling process.

To explain the effect of pH on the process, without inter-electrode insulation, note that locally at the anodically polarised steel band surface, metal ions (Fe, Cr and Ni) are released into the solution as a consequence of the oxide/metal dissolution. As the metal ions migrate through the solution they tie up the hydroxyl ions, produced at the cathodes, yielding hydroxides, all of which except $Ni(OH)_2$ have very low solubility.[21] This phenomenon as well as the production of protons as a result of hydrolysis of water makes the solution at the anodic steel band surface acidic, which is said[12] to promote chemical dissolution of the oxide. At the cathodically polarised steel band surface, the environment becomes alkaline as a result of hydrolysis of water yielding hydroxyl ions. The otherwise hard to dissolve silica, SiO_2, is dissolved in a very alkaline environment.[13]

More specifically, the production of protons H^+ and hydroxyl ions OH^- at the anodes and cathodes, respectively, is proportional to the strength of the current densities at the respective electrode. A separation between the anodes and cathodes into different compartments would yield an imbalance between the produced H^+ and OH^- ions, which would result in a global increase in the pH and consequent alkaline environment in the cathode compartments and a possible global decrease of the pH with a consequent acidic environment in the anode compartments. This could affect and alter the reactions actually occurring as described above.

In addition it is known[19] that in an alkaline environment Fe(III) ions yield through hydrolysis a red brownish jellylike substance, probably FeO(OH) forming undesirable sludge, which has also been observed to linger close to the electrode surfaces, insulating them and reducing the mass transport to the electrode surface as well as the conductivity. This substance is soluble in acidic solutions, but to a very small extent in alkaline solutions. As described above, with complete separation of the compartments all metal ions (Fe, Cr and Ni) resulting from the dissolution of the oxide/base metal on the anodic sections of the steel band would then accumulate in only one compartment, instead of being evenly distributed throughout the whole pickling tank. Therefore, because of the pH increases in the compartment where the metal ions accumulate, i.e. in the cathode compartment and consequently where the band is anodic, the described jellylike substance formed here would not dissolve. Altogether this would tend to decrease the efficiency of the pickling process. Cr ions are also observed to yield the same sludge producing effect as Fe ions, but not as pronounced. It can be seen that concentration and pH changes that occur as a consequence of electrode separation promote different reactions from the ones occurring in the electrolytic pickling process where the electrodes are not separated.

Furthermore, the active metal ions, produced by the electrochemical dissolution of the oxide/base metal, react by hydrolysis in the electrolyte and form metal hydroxides. The hydroxides precipitate as sludge and accumulate in the anodic compartment where electrolytic pickling occurs, and none accumulate in the cathodic compartment. Lack of mixing of the electrolyte owing to such separation decreases the lifetime of the electrolyte and necessitates more frequent process stops for sludge disposal. Altogether, these disadvantages of a complete separation of the electrodes might lead to a loss in pickling efficiency, outweighing the advantage of the elimination of the inter-electrode short-circuiting current.

Another problem in bipolar pickling of stainless steel bands is that the bottom side of the steel band is in general more poorly pickled.[1] It is therefore preferable to find a way of applying different pickling intensities on the top and bottom sides of the steel band. This, however, is impossible to do with the present configuration of the industrial pickling tanks.

To remedy the previously described problems causing low current and energy efficiencies and poor pickling, this paper proposes and outlines the method[1] of inter-electrode insulation that was developed and successfully tested to reduce or eliminate the inter-electrode short circuit. The method was shown both theoretically and experimentally to significantly increase the current efficiency and also to reduce the energy consumption of the electrolytic pickling process. Furthermore, one can design the insulating partitions to allow a partial opening between the electrodes adjusted for applying appropriate electrolyte mixing, and perhaps for adjusting the pickling intensity between the top and bottom parts of the band.

Experimental apparatus and procedure

The cell used for electrolytic pickling experiments without inter-electrode insulation is shown in Fig. 4*a*. It consisted of a rectangular $360 \times 235 \times 260$ mm glass tank (1), containing two sets of electrodes, made of three lead anodes (2) and three stainless steel cathodes (3), placed symmetrically above and below the stationary steel band, which was supported by two Plexiglas holders (4), a regulated 1 kW DC power supply, a calibrated 1–10 V ($\pm 0{\cdot}5\% + 1$ dgt) voltmeter and 1–10 A ($\pm 1{\cdot}5\% + 5$ dgts) current meter, all immersed in a solution of neutral sodium sulphate (7). While the industrial process typically uses three electrode groups, the choice of two or three electrode groups does not affect the understanding or function of the process or the current efficiency at these current densities. Two groups of electrodes (cathode–anode) instead of three (cathode–anode–cathode) were chosen in the laboratory cell to be able to study separately the effect of the anodic/cathodic electrode reactions at the steel band surface, i.e. distinguish between the different polarised sections (experimental results of the pickling of the steel band in the different anodic–cathodic sections are shown and discussed in the section on 'Evaluation of results' below).

Oxidised type 304 and 316 stainless steel bands (5), $300 \times 50 \times 3$ mm, annealed at the AvestaPolarit AB annealing and pickling line, were used. The cell was placed on two magnetic plates for activating the magnetic stirrers, at the bottom of the tank, which could be used to stir the solution when wished. The temperature in the cell was kept at 21°C.

To allow measurement of the current passing through the steel band, it was cut across its centre in two halves, and stainless steel rods, type 304 of diameter 4 mm and

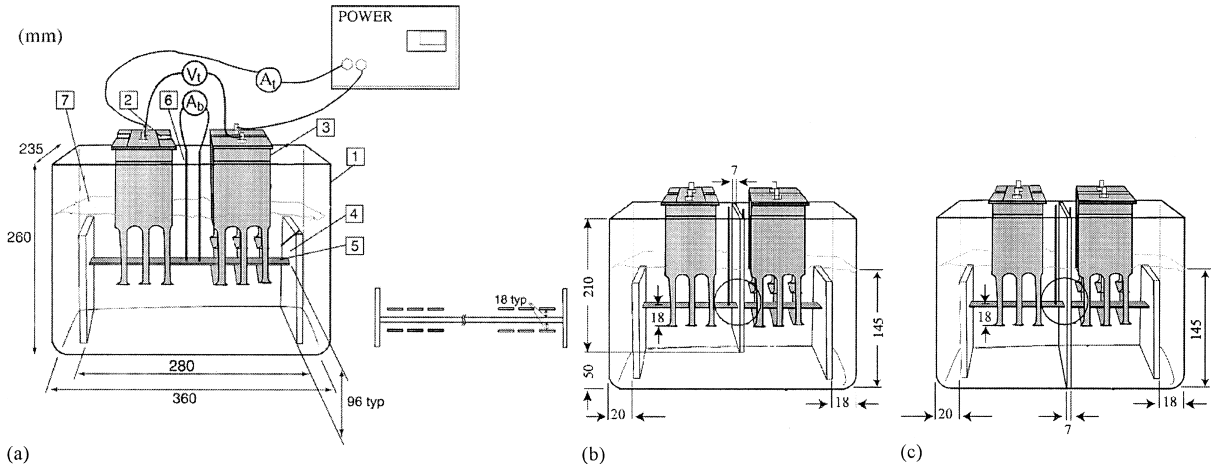

experimental cell – 1: container (glass, 360 × 235 × 260 mm), 2: anodes (lead), 3: cathodes (stainless steel), 4: supports (insulating Plexiglas), 5: steel band (316, 300 × 50 × 3 mm), 6: current measurement extension steel rods (304), 7: the electrolyte, aqueous sodium sulphate solution; the magnified details in the upper right corner show two views of the electrode to band arrangement and distance (in mm): the voltmeter (V_t) measures the electrode potential; the ammeter (A_b) measures the total current, and the current passing through the steel band

4 *a* the experimental cell without inter-electrode insulation; *b* the experimental cell with partial insulation between the electrodes, and *c* with complete insulation between the electrodes

resistance $R=0{\cdot}0014\ \Omega$ (6) were screwed on to each of the halves. The two halves were attached end to end by 3 mm silicon cement between them. This way the current that passed through the steel band was forced through the steel rods and through a current meter. The technique is described in Fig. 5.

The improvement in the electrolytic process was accomplished and tested by introducing a Plexiglas insulator between the electrodes of different polarity, Fig. 4*b*. The insulator was 7 mm thick and served to electrically isolate the anodes from the cathodes, partially in some of the experiments and completely in the others.

In the case where a partial insulator was used, a Plexiglas plate 235 × 210 mm was attached to walls, between the electrodes, of the cell by silicon cement, down to about 50 mm from the bottom of the cell, leaving this 50 mm gap free, with the electrolyte continuously connecting the separated parts of the cell in it. The cross sectional area above the steel band was completely insulated, but the area below the steel band was only partly insulated, leaving about 66% of the cross sectional area of the cell free of insulation. Also here, the steel band was cut across its centre in two halves to each of which stainless steel rods were screwed. The two halves were then inserted into a 50 × 3 mm slit, cut out in the Plexiglas plate, about 45 mm from the bottom of the plate and attached end to end by 3 mm silicon cement between them. As previously described, the current passing through the steel band was forced through the steel rods and through the current meter.

When complete insulation was used, a 235 × 260 mm Plexiglas plate was attached by silicon cement to the walls and bottom of the cell between the electrodes. The steel band used was prepared similarly to the previous descriptions and inserted into a 50 × 3 mm slit, cut out in the Plexiglas plate, about 93 mm from the bottom of the plate, and attached end to end by 3 mm silicon cement between them. Here, consequently, the inter-electrode area was completely (100%) insulated, as shown in Fig. 4*c*.

Experiments were conducted with the electrode to band distance set as shown in Table 2, dictated by the size limitations of the experimental cell. The measurement procedure in all three cases was to increase the cell voltage from 1 to 10 V, and simultaneously measure the total current through the electrodes and through the steel band, to evaluate the achieved improvement in process efficiency in relation to the insulated area.

The concentration of active component Fe, Cr and Ni ions, in the electrolyte throughout the pickling cell is proportional to the amount of pickling and it was therefore measured as different degrees of inter-electrode insulation were applied and compared to the concentration in the uninsulated setup. When the original cell was used, i.e. the case with no applied insulation, the samples were taken from an arbitrary position in the tank. In the other cases, the solution samples were taken from both the anodic and cathodic compartments of the tank. The Fe ion concentration was analysed by titration and the Cr and Ni ion contents were analysed by inductive

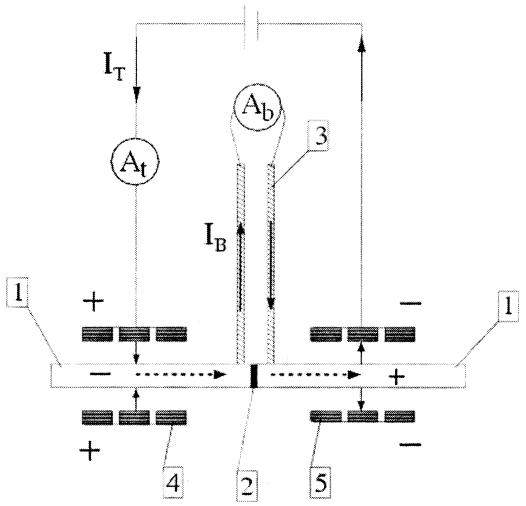

1: steel band; 2: 3 mm silicon cement; 3: stainless steel rod; 4: anodes; 5: cathodes

5 Technique for measuring the current in the steel band

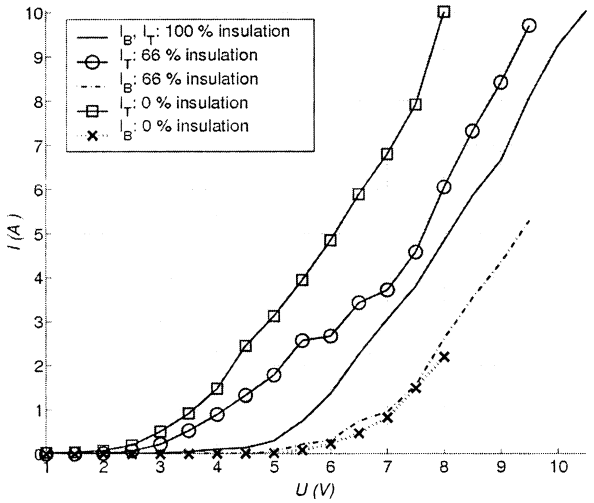

6 Current *I* *v.* potential *U* plots: comparison of the measured total I_T and band I_B currents with no (0%), partial (66%) and complete (100%) inter-electrode insulation

coupled plasma (Thermo Javell Ash, Iris/AD, AES-ICP) equipment at AvestaPolarit AB. The ICP measurement errors are shown in Table 3.

Evaluation of results

Experiments were conducted to determine the effects of inter-electrode insulation on the current efficiency and the results are shown here.

A comparison of the measured total current I_T and the current passing through the steel band I_B in the three cases studied with no insulation (0%), partial insulation (66%) and complete insulation (100%) between the electrodes is shown in Fig. 6.

Because current passes where it encounters the least resistance, most of it passes directly through the electrolyte between the electrodes when no insulation exists between them and largely bypasses the steel band to be pickled. As seen in Fig. 6, the current passing through the steel band is only about 20% of the total applied current. When the inter-electrode area was

Table 1 Parameters used in the numerical analysis: here Δ_{eb} denotes the electrode to band and Δ_{ie} the inter-electrode distances in the model

δ	3 mm
Δ_{eb}	20 mm
ε	5 mm
Δ_{ie}	50 mm
H	50 mm
d	1·5 mm
L_a, L_c	20 mm
L	300 mm
κ_e[21]	9·08 S m^{-1}
κ_a, κ_b, κ_c	1×10^{7} S m^{-1}
T	294 K
pH (anodes), pH (cathodes)	1, 13
α_{H_2} (Ref. 22)	0·5
α_{O_2} (Pb)[23], α_{O_2} (Fe)[24]	0·55, 1·5
i_{0,O_2} (Pb),[23] i_{0,O_2} (Fe)[24]	1×10^{-14} Am^{-2}, 1×10^{-6} Am^{-2}
i_{0,O_2} (Ref. 22)	1×10^{-2} Am^{-2}
Θ	0·2
E^0_{O2} (Ref. 23)	1·229 V
E^0_{H2} (Ref. 23)	−0·8281 V
V_a, V_c	±6 V

Table 2 Parameters of the experiment. In column 2 $\Delta_{eb,top}$ and $\Delta_{eb,bottom}$ denote top and bottom electrode to band distances respectively in the experiment

δ, ε, mm	$\Delta_{eb,top}$, $\Delta_{eb,bottom}$, mm	Δ_{ie}, mm	H, d, mm	$L_{a,c}$, mm	L, mm
3, 5	18, 20	50	50, 1·5	20	300

insulated partially to about 66% (as described above), the current through the steel band was about 55% of the total applied current. A complete insulation of the inter-electrode area yielded a current efficiency of 100%. In this case the total current was forced through the steel band.

From the plots in Fig. 6 it is also seen that for a specific cell voltage, the total current is lower when the inter-electrode insulations are inserted. This can be somewhat explained by the increase in the resistance in the electrolyte when the insulations are employed. The resistance in the electrolyte is l_e, expressed as follows $R_e=l_e/A\kappa_e$ (Ω), where l_e (m) is the distance between the selected points in the electrolyte, A (m^2) is the cross section area and κ_e (Sm^{-1}) is the conductivity of the electrolyte. Therefore, when l_e is selected to be the inter-electrode distance, it is seen from R_e that decreasing the open cross-section area will increase the resistance in the electrolyte.

The observed lower current density tends to have a positive effect on the process because it also reduces the amount of produced gas, explained in more detail as follows. The production rate of gas $\dot{m}$ (kg s^{-1}), can be expressed as $\dot{m}=\dot{r}M$, where $\dot{r}$ (mol s^{-1}) is the molar gas production rate, and M (kg mol^{-1}) is the molar weight of the produced species. In turn, $\dot{r}$ is proportional to the current density, according to Faraday's law, $\dot{r}=(\boldsymbol{i}\cdot\boldsymbol{n})A/zF$ (mol s^{-1}) where $\boldsymbol{i}$ is the current density vector because of the gas production reaction, $\boldsymbol{n}$ is the unit vector normal to the surface where the gas is produced, A is the surface area (m^2), z the number of electrons transferred in the reaction and F is Faraday's constant. Here for example, at the same applied cell voltage $U=8$ V, the total current density is reduced from about 0·4 kA m^{-2} with no insulation to about 0·24 kA m^{-2} with partial insulation, and to about 0·2 kA m^{-2} with complete insulation. Using this theory, it translates into electrode gas production reductions of 40% and 50% for partial and complete insulations respectively. At the same time, however, the amount of gas produced at the steel band increases, as a result of an increase in the current through the steel band at 8 V from 2·2 A (no insulation) to 2·62 A (partial insulation) and to 4·84 A (complete insulation), by about 20% and 120% for partial and complete insulations respectively. The fractional bubble

Table 3 Measurement errors of the Cr and Ni ion concentration (using the inductive coupled plasma analyser)

Range, mg l^{-1}	Error estimate, mg l^{-1}	Percentage
0–0·5	±0·05	±10
0·5–5	±0·1	±20–2
5–20	±0·5	±10–2·5
20–100	±1·0	±5–1

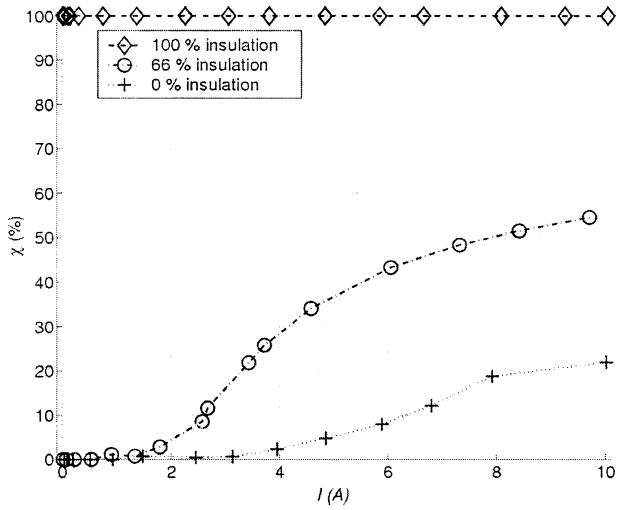

7 Current efficiency χ (%) versus the total applied current I_T (A), for the case with no (0%), partial (66%) and complete (100%) inter-electrode insulation

coverage Θ of the electrode surfaces is stated to be proportional to the current density i as $\Theta \approx i^{0.18}$ (Ref. 20). According to this relation, the observed decrease in the total current density from 0·4 to 0·2 kA m^{-2} yields 12% lower surface coverage at the electrodes. At the steel band surface, however, the bubble coverage increases by about 15% owing to the increase in the current density from about 0·15 to 0·32 Am^{-2} at the steel band surface at the same time. The authors' analysis[10] predicts that the observed decrease in the total current density at 8 V, using no insulation compared to complete insulation, would yield an increase of about 8% in the effective electrolyte conductivity. With a partial insulation compared to no insulation, the bubble coverage increases about 3% according to the above relation. In conclusion the partial insulation will be more beneficial in relation to the relatively marginal increase in gas production and surface coverage of bubbles at the steel band surface compared to the corresponding increase with complete insulation.

As seen in Fig. 6, the presence of insulation also has a positive effect in that it lowers the threshold voltage at which current starts passing through the steel band, from about 5 V when no insulation is applied to about 4 V when 100% insulation is applied. This is indeed plausible, because the current density at the band increases when the insulation is applied, resulting in a higher overpotential and consequently an activation of the reactions at a lower voltage.

Figure 7 shows that the current efficiency at I=10 A increases by about 250% for 66% insulation and 450% for 100% insulation. Consequently, the current density at the steel band surface, based on its anodic polarised half surface, increases from about 0·15 kA m^{-2} with no insulation to about 0·37 kA m^{-2} with 66% insulation, and further to about 0·67 kA m^{-2} with 100% insulation. Assuming that the pickling rate is proportional to the band current density, it increases by the same amounts, but the actual relation between the amount of current going to oxide scale dissolution and gas production is not totally clear.

Figure 8 shows photographs of the electrolytic experiment running with different degrees of inter-electrode insulation.

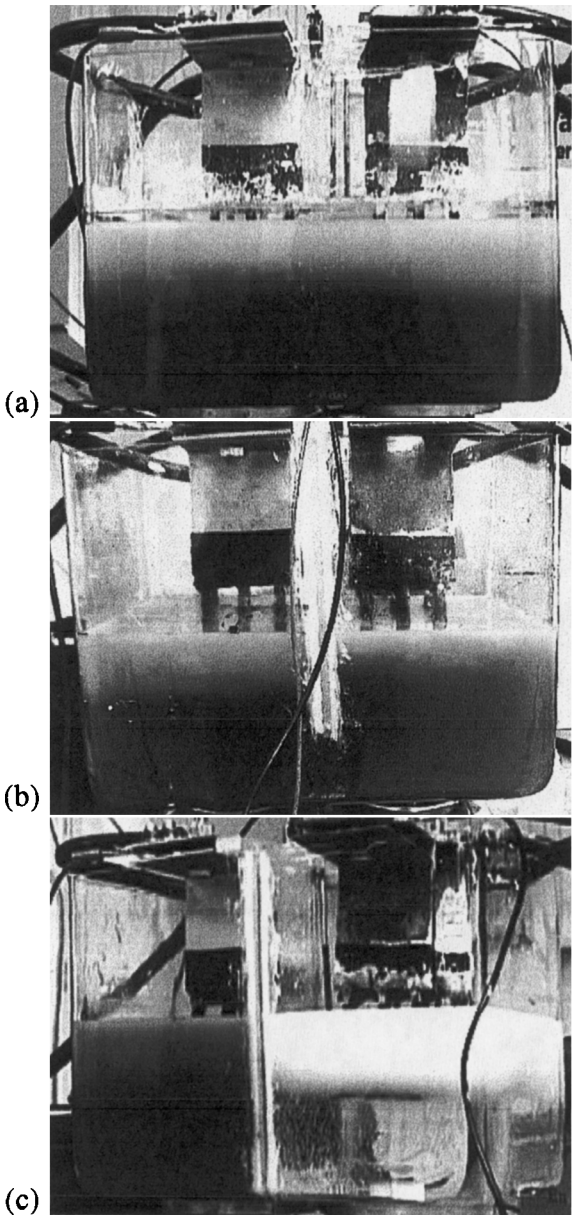

left half cathode and anodically polarised band half; *right half* anode and cathodically polarised band half.
a 0% inter-electrode insulation; solution is fairly homogeneous, the lighter colour vertical strips near the left and right sides inside the solution are the steel band supports, *b* 66% inter-electrode insulation; a thicker layer of produced gas is seen in the cathodic section, to the left, *c* 100% inter-electrode insulation; there is an even thicker layer of produced gas in the cathodic compartment, to the left, the solution under it appears dark because of the increased amount of sludge accumulating there, as a result of complete inter-electrode insulation, but it is also an artifact of the illumination during the photography

8 Photograph of the pickling process with $\Delta_{eb,top}$= 18 mm, $\Delta_{eb,bottom}$=20 mm, Δ_{ie}=50 mm, $c_{Na_2SO_4}$=170 g l^{-1}, i=0·46 kA m^{-2} and T=294 K

In Fig. 8*a* and *b*, where no insulation and partial insulation was used respectively, the electrolyte solution appears homogeneous. It is concluded that a partial insulation does not alter the concentration distribution in the electrolyte, as further proven by concentration measurements described below. However, with a complete inter-electrode insulation, Fig. 8*c*, a clear

difference in the electrolytes in the two cell compartments is seen. This clearly shows that dissolution of oxide/base metal is confined to the anodic section of the steel band. Note, that even though the figure does not show the bubbles as clearly in the anodic compartment as in the cathodic one, they are nevertheless equally present. Therefore with this configuration the dissolved metal ions and sludge accumulate in only one cell compartment, i.e. the one where the steel band is anodically polarised. As discussed above, it is preferable to have a homogeneous distribution of the dissolved metal ions and sludge in the whole pickling cell, to avoid changes in the process chemistry and pH and frequent sludge removal.

To establish how the different degrees of insulation affect the metal ion concentration in the pickling cell, samples of the electrolyte solution in the different cell compartments, seen in Fig. 8, were taken out at different times and analysed for their ion content. The results of these analyses are shown in Fig. 9.

As a result of the electrochemical dissolution reactions of the oxides Cr_2O_3, Fe_2O_3 and NiO, and probably some base metal dissolution, Cr, Ni and Fe ions are formed in the electrolyte solution and ultimately react by hydrolysis forming metal hydroxides (sludge), which are disposed of. The results of the analysis shown in Fig. 9 can be summarised as follows.

1. After 4 h of pickling the concentration of Cr ions had increased, with no insulation (Fig. 9*a*) by 40%, with partial (66%) insulation by 170%, and with complete (100%) insulation by 420%. Similarly the concentration of Ni ions (Fig. 9*b*) had increased, with no insulation by 250%, with partial insulation by 470%, and with complete inter-electrode insulation by 780%. It is concluded that the concentration of metal ions, indicative of the extent of pickling, increases with time and degree of inter-electrode insulation in the pickling cell

2. With a partial inter-electrode insulation, the Cr concentration, Fig. 9*a*, after 15 min is 33% higher than in the no-insulation case, and the Ni ion concentration, Fig. 9*b*, is 80% higher. Clearly the rate of dissolution of both chromium and nickel oxide increases as the degree of inter-electrode insulation, and consequently the current density at the steel band surface increases. Even with a partial insulation it is seen that a significant increase in the pickling rate is achieved. Consequently, a greater amount of sludge also will have to be accounted for, and good mixing of the electrolyte would be desirable when insulations are inserted

3. With no or partial inter-electrode insulation, the concentration of Cr and Ni ions in the cathodic and anodic sections of the cell were the same, Fig. 9*a*, revealing that the electrolyte is well mixed, as desired. However, as seen in Figs 9*b* and *c*, with a complete insulation the Cr and Ni ion concentration in the cathodic cell compartment (i.e. where the steel band is cathodic) is zero, indicating that no pickling occurred there. Consequently, these ions accumulate in the anodic compartment of the cell. This concentration non-uniformity affects the pickling process negatively as was discussed in the introduction and may reduce the benefit of the increased pickling rate, which complete inter-electrode insulation produces.

4. The concentration of Cr ions (Fig. 9*a*) is higher than of the Ni ions (Fig. 9*b*) and Fe ions (Fig. 9*c*) in the electrolyte, indicating that chromium oxide was

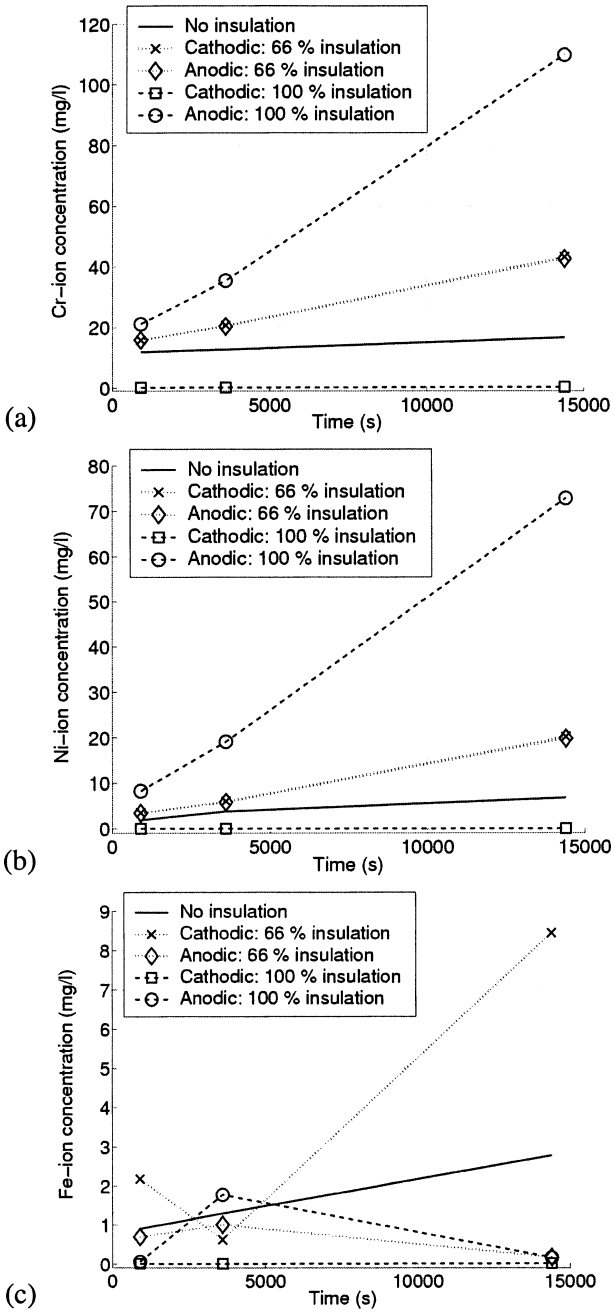

a Cr ions; *b* Ni ions; *c* Fe ions: here it is noted that the measured Fe values are within the titration measurement method error band

9 The ion concentration variation in the electrolyte as a function of time: in cell with no insulation the samples were taken randomly from the bottom; in cell with partial and complete inter-electrode insulations the samples were taken from the anodic and cathodic cell compartments

dissolved to a greater extent than nickel oxide and iron oxide. It is also seen that as the current density at the steel band surface increases, i.e. with increasing degree of insulation NiO tends to dissolve to a greater extent. From Fig. 9*c*, it is seen that the magnitude of Fe ions is almost 10 times lower than that of the other ions.

5. With a partial inter-electrode insulation, the Cr concentration, Fig. 9*a*, after 15 min is 33% higher than in the no-insulation case, and the Ni ion concentration, Fig. 9*b*, is 80% higher. Clearly the rate of dissolution of both chromium and nickel oxide increases as the degree

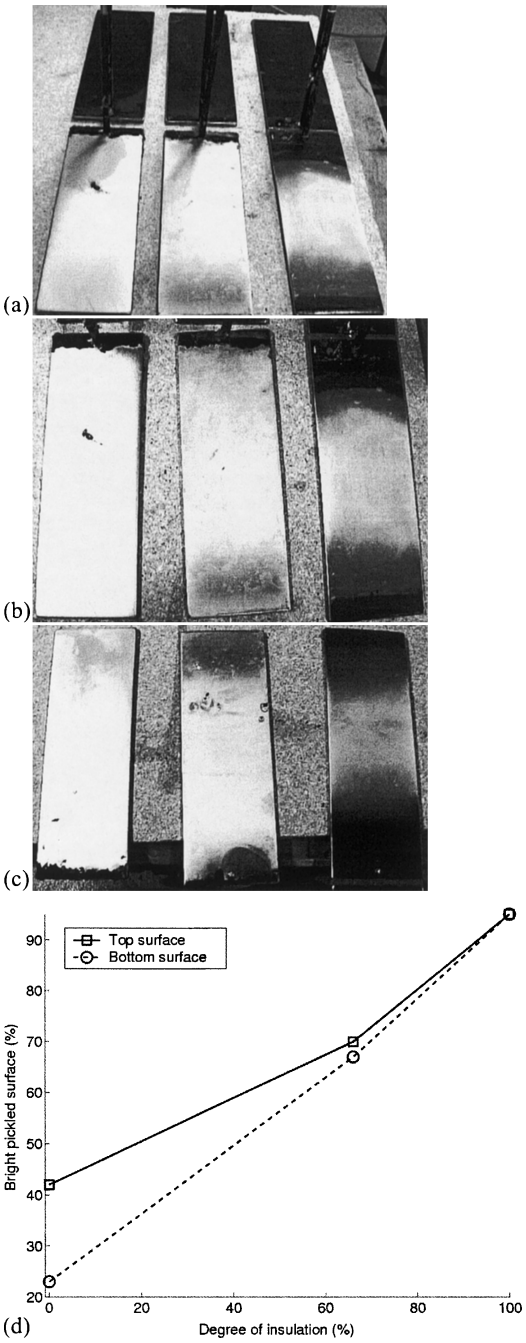

left steel band: pickled with 100% insulation; *centre steel band*: pickled with 66% insulation; *right steel band*: pickled with no insulation
a top view of both anodic (the brighter bands at the bottom of the photograph) and cathodic (the darker ones) polarised sections of the steel band; *b* close-up of the top surface of the anodic polarised steel strip section; *c* close-up of bottom surface of the anodic polarised steel strip section; *d* degree of removed oxide (%) as function of inter-electrode insulation extent (%): in *a–c*, brighter regions indicate better pickling and the darkest areas indicate the oxide layer

10 Photographs and pickled area measurements of steel bands pickled electrolytically for 4 h, $\Delta_{eb,top}$=18 mm, $\Delta_{eb,bottom}$=20 mm, Δ_{ie}=50 mm, $c_{Na_2SO_4}$=170 g l^{-1}, i=0·46 kA m^{-2}, T=294 K

of inter-electrode insulation, and consequently current density at the steel band surface, increases. Even with a partial insulation it is seen that a significant increase in the pickling rate is achieved.

Figure 10 shows photographs of the steel bands pickled for 4 h with 100% insulation (left), 66% insulation (centre), and no insulation (right).

In Fig. 10*a* it is seen that the oxide scale on the section of the steel band that was cathodically pickled has not been affected, as expected. The anodically polarised section of the steel band is pickled to different degrees depending on the extent of inter-electrode insulation.

The degree of pickling and of the pickling uniformity is seen (Fig. 10*b–d*) to increase with the extent of inter-electrode insulation. In general, the bottom surface is usually more poorly pickled than the top surface, as seen by comparing Fig. 10*b* and *c*, and displayed in Fig. 10*d*, which shows a rough estimate (by measuring the pickled area) of the effect the inter-electrode insulation on the pickling of the steel band surface.

Conclusions

To validate the prediction that inter-electrode insulation improves the electrolytic pickling efficiency, experiments were conducted in a small experimental electrolytic pickling cell with varying degree of the insulation. Some of the main results follow.

1. The inter-electrode short circuit current is indeed reduced and in fact eliminated with complete insulation, whereby the current efficiency of the process is improved from 20% without insulation to 100% with.
2. Complete insulation between the electrode groups yields 100% current efficiency, but the sludge is accumulated in the compartments where the steel band is anodic, resulting in an inhomogeneous electrolyte and higher maintenance requirements.
3. Use of an insulation which covers less, say 66%, of the electrolyte cross section area between the anode and cathode electrode groups, results in a significant improvement in the process efficiency while at the same time maintaining good circulation and homogeneity of the electrolyte solution.
4. The method is relatively easily applicable as a retrofit to existing electrolytic pickling tanks and the cost is relatively low, saving investments in new equipment.
5. Partial adjustable insulations give a valuable operational flexibility in the pickling tank, when steel bands of different grades are being pickled; for example, when the steel bands have a thick but easy to pickle scale, which generates much sludge, the insulation could be adjusted to provide a larger electrolyte passage between the electrodes and allow higher mixing and homogeneity of the solution. When the steel band to be pickled has a thin but hard to pickle scale, the insulation can be adjusted to insulate most or all of the inter-electrode cross section area.

Appendix

Nomenclature

A	electrode area (m^2)
d	steel band half thickness (mm)
$c_{Na_2SO_4}$	concentration of the electrolyte solution ($g\ l^{-1}$)
E	potential difference between the electrode and adjacent solution (V)
E_0	equilibrium potential (V)

E_{0,Cr_2O_3} equilibrium potential of chromium oxide dissolution (V)
$E_{0,Fe}$ equilibrium potential of hydrogen evolution (V)
E_{0,O_2} equilibrium potential of oxygen evolution (V)
$E^0_{H_2}$ standard potential of hydrogen evolution (V)
$E^0_{O_2}$ standard potential of oxygen evolution (V)
F Faraday constant (96485 $C\ mol^{-1}$)
H height of the free electrolyte surface (mm)
I_T experimentally measured total current (A)
I_B experimentally measured current passing through the steel band (A)
i current density ($A\ m^{-2}$)
i_{0,H_2} exchange current density of the hydrogen evolution reaction ($A\ m^{-2}$)
i_{0,O_2} exchange current density of the oxygen evolution reaction ($A\ m^{-2}$)
l_e arbitrary length (m)
L steel band length (mm)
L_a anode length (mm)
L_c cathode length (mm)
L_e distance between points in electrolyte (m)
M molar weight of a species ($kg\ mol^{-1}$)
$\dot{m}$ mass rate of production ($kg\ s^{-1}$)
$\boldsymbol{n}$ normal unit vector
R steel rod resistance (Ω)
R_e electrolyte resistance (Ω)
$\dot{r}$ molar rate of production ($mol\ s^{-1}$)
T absolute temperature (K)
U cell voltage (V)
V_a applied anodic potential (V)
V_c applied cathodic potential (V)
z number of electrons transferred in a electrochemical reaction

α_{H_2} transfer coefficient for the hydrogen reaction
α_{O_2} transfer coefficient for the oxygen reaction
δ thickness of the anodes and cathodes (mm)
ε inner anode-anode and cathode-cathode spacing (mm)
Δ_{eb} electrode-to-band distance (mm)
$\Delta_{eb,top}$ top electrode-to-band distance (mm)
$\Delta_{eb,bottom}$ bottom electrode-to-band distance (mm)
Δ_{ie} inter-electrode distance (mm)
ηS surface overpotential (V)
κ_α anode conductivity ($S\ m^{-1}$)
κ_b steel band conductivity ($S\ m^{-1}$)
κ_c cathode conductivity ($S\ m^{-1}$)
κ_e electrolyte conductivity ($S\ m^{-1}$)
Θ surface blockage of bubbles
χ current efficiency, $\chi = I_B/I_T$

Subscripts

a anode
b steel band
Cr_2O_3 chromium oxide
c cathode
e electrolyte
Fe iron
H_2 hydrogen
0 equilibrium value
Na_2SO_4 electrolyte solution
O_2 oxygen

Acknowledgements

This work has been conducted at the Faxén Laboratory of the Royal Institute of Technology (KTH). The counsel of Professor Fritz Bark, Director of the laboratory, and the partial financial support of AvestaPolarit AB are gratefully acknowledged.

References

1. 'Method and device in connection with pickling', Patents WO 02/33154 A1 (25 April 2002), EP1332245 and SE519159, 21 April 2002.
2. 'Process and apparatus for producing strip products from stainless steel', Patent US 5804056, 8 September1998.
3. S. A. Bradford: in 'Metals handbook', 9th edn, Vol. 13, 62–76; 1987, Metals Park, OH, ASM.
4. E. Braun: *Iron Steel Eng.*, 1980, **57**, (4), 79–81.
5. E. T. Shapovalov, A. P. Shlyamnev, E. A. Ulyanin, V. D. Nikitin, A. R. Fisher, D. B. Goldzon, L. V. Popova and I. I. Milovanov: *Steel USSR*, 1982, **12**, 215–219.
6. V. I. Ignat'ev, N. N. Sergeeva and M. A. Shluger: *Zh. Prikl. Khim.*, 1987, **60**, 278–282.
7. J. M. K. Hildén, J. V. A. Virtanen and R. L. K. Ruoppa: *Mater. Corros.*, 2000, **51**, 728–739.
8. V. I. Dunaevskii, V. T. Stepanenko, M. Ya. Shnol and L. N. Bespal'ko: *Protect. Met.*, 1985, **21**, 359–363.
9. Anon.: *Sheet Metal Ind.*, 1979, **56**, (1), 36, 39, 40, 42.
10. N. Ipek: 'Modeling of electrolytic pickling', Licentiate thesis, Stockholm: Tekn. Högsk., Mechanics Department, Sweden, 2002.
11. E. T. Shapovalov, G. V. Kazakova and N. V. Andrushova: *Steel USSR*, 1983, **13**, 27–31.
12. D. Henriet: 'Surface treatments for stainless steel state of the art – developments and trends', Final report, EUR 17248 EN, Office for Official Publications of the European Communities, Luxembourg, 1996, 329 pp.
13. M. Pourbaix: 'Atlas of electrochemical equilibria in aqueous solutions', (trans. J. A. Franklin), 2nd edn; 1974, Houston, TX, National Association of Corrosion Engineers.
14. L.-F. Li and J.-P. Celis: *Can. Metall. Q.*, 2003, **42**, 365–376.
15. Y. Kawabata, S. Owada, S. Satoh, F. Togashi, O. Hashimoto, S. Kakihara and T. Kawasaki: in Eur. Stainless Steel Conf. 'Processes and materials innovation stainless steel', Florence, Italy, October 1993, Vol. 2, 2.83–2.87.
16. M. Ito, M. Yoshioka, Y. Seino, M. Suzuki, M. Sakuta, Y. Maki and Y. Kawabata: *ISIJ Int.*, 1997, **37**, 391–398.
17. 'Method for removal of films from metal surfaces using electrolysis and cavitation action', Patent S 5795460, 18 August 1998.
18. 'Method and device for pickling and galvanizing', Patent US 5449447, 12 September 1995.
19. G. Hägg: 'Allmän och oorganisk kemi', 7th edn; 1963, Almqvist & Wikseoll, Stockholm.
20. H. Vogt: *J. Appl. Electrochem.*, 1983, **13**, 87–88.
21. 'Handbook of chemistry and physics', 67th edn; 1986–1987, CRC Press, Boca Raton, FL.
22. R. N. O'Brien and P. Seto: *J. Electrochem. Soc.*, 1970, **117**, (1), 32–34.
23. C. Wenmi and G. Bingkun: *J. Central South Univ. Technol.*, 1997, **4**, (1), 69–72.
24. J. O'M. Bockris and A. K. N. Reddy: 'Modern electrochemistry', 1st edn, Vol. 2; 1970, New York, Plenum Press.